# ORGANOMETALLICS

Article

# Competing Pathways in the Photochemistry of Ru(H)₂(CO)(PPh₃)₃

Barbara Procacci,[†,‡] Simon B. Duckett,*,[†,‡] Michael W. George,*,[§,∥] Magnus W. D. Hanson-Heine,[§] Raphael Horvath,[§] Robin N. Perutz,*,[†] Xue-Zhong Sun,[§] Khuong Q. Vuong,[§] and Janet A. Welch[†]

[†]Department of Chemistry, University of York, York YO10 5DD, U.K.

[‡]Centre for Hyperpolarisation in Magnetic Resonance, Department of Chemistry, York Science Park, University of York, York YO10 5NY, U.K.

[§]School of Chemistry, University of Nottingham, Nottingham NG7 2RD, U.K.

[∥]Department of Chemical and Environmental Engineering, The University of Nottingham Ningbo China, 199 Taikang East Road, Ningbo 315100, People's Republic of China

Ⓢ *Supporting Information*

**ABSTRACT:** The photochemistry of Ru(H)₂(CO)(PPh₃)₃ (**1**) has been reinvestigated employing laser and conventional light sources in conjunction with NMR spectroscopy and IR spectroscopy. The sensitivity of NMR experiments was enhanced by use of *p*-H₂-induced polarization (PHIP), and a series of unexpected reactions were observed. The photoinduced reductive elimination of H₂ was demonstrated (a) via NMR spectroscopy by the observation of hyperpolarized **1** on pulsed laser photolysis in the presence of *p*-H₂ and (b) via nanosecond time-resolved infrared (TRIR) spectroscopy studies of the transient [Ru(CO)(PPh₃)₃].



Elimination of H₂ competes with photoinduced loss of PPh₃, as demonstrated by formation of dihydrogen, triphenylarsine, and pyridine substitution products which are detected by NMR spectroscopy. The corresponding coordinatively unsaturated 16-electron intermediate [Ru(H)₂(CO)(PPh₃)₂] exists in two isomeric forms according to TRIR spectroscopy that react with H₂ and with pyridine on a nanosecond time scale. These two pathways, reductive elimination of H₂ and PPh₃ loss, are shown to occur with approximately equal quantum yields upon 355 nm irradiation. Low-temperature photolysis in the presence of H₂ reveals the formation of the dihydrogen complex Ru(H)₂(η²-H₂)(CO)(PPh₃)₂, which is detected by NMR and IR spectroscopy. This complex reacts further within seconds at room temperature, and its behavior provides a rationale to explain the PHIP results. Furthermore, photolysis in the presence of AsPh₃ and H₂ generates Ru(H)₂(AsPh₃)(CO)(PPh₃)₂. Two isomers of Ru(H)₂(CO)(PPh₃)₂(pyridine) are formed according to NMR spectroscopy on initial photolysis of **1** in the presence of pyridine under H₂. Two further isomers are formed as minor products; the configuration of each isomer was identified by NMR spectroscopy. Laser pump-NMR probe spectroscopy was used to observe coherent oscillations in the magnetization of one of the isomers of the pyridine complex; the oscillation frequency corresponds to the difference in chemical shift between the hydride resonances. Pyridine substitution products were also detected by TRIR spectroscopy.
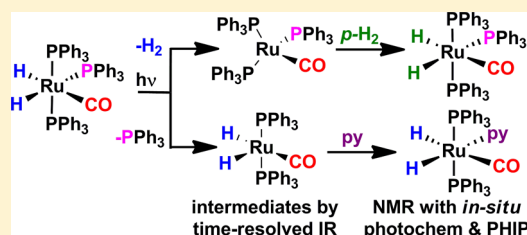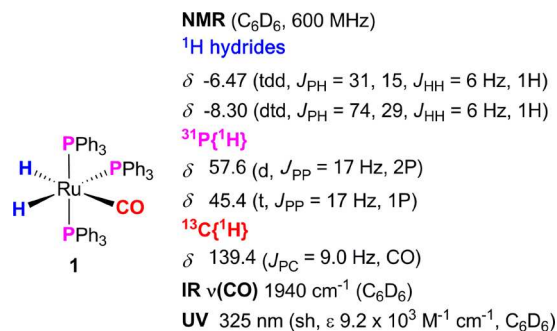
## ■ INTRODUCTION

Photochemical methods offer low-temperature routes to synthesis, excellent routes to study reaction mechanisms, and great opportunities for catalysis. Indeed, there has been a great resurgence of interest in photocatalysis.[1−3] Metal hydrides play a major part in the photochemistry of organometallics and coordination complexes, and we have recently reviewed their behavior systematically.[4] One of the earliest metal hydrides to be studied photochemically was Ru(H)₂(CO)(PPh₃)₃ (**1**) (Scheme 1), a compound of great interest for its catalytic properties both under illumination and by thermal means.[5−13] The original studies of its photochemistry demonstrated loss of H₂, but not CO, on irradiation in benzene. Selectivity for loss of H₂ over loss of CO is now recognized for several metal carbonyl dihydrides.[14] When **1** was photolyzed in benzene solution under a CO atmosphere, Ru(CO)₃(PPh₃)₂ was formed, leaving the sequence in which H₂ and PPh₃ had been dissociated and CO coordinated uncertain.[5] In 1997, we

identified **1** as an excellent target for investigating the photodissociation of H₂ by time-resolved UV/vis and time-resolved IR spectroscopy.[15] We observed a transient by both techniques that was assigned to [Ru(CO)(PPh₃)₃] and measured its rate of reaction with H₂ ((8.4 ± 0.4) × 10⁷ dm³ mol⁻¹ cm⁻¹ at room temperature). It was of particular importance that the transient exhibited a 95 cm⁻¹ shift to low frequency in its CO-stretching band, providing proof of H₂ loss. Moreover, ultrafast spectroscopy demonstrated that it was formed within the response time of the instrument of 6 ps. The only other transient observed by IR spectroscopy had a significant rise time, suggesting that it was a secondary product. Thus, we concluded that there was ultrafast and concerted photochemical reductive elimination of H₂ from Ru(H)₂(CO)-(PPh₃)₃. As we now show, this study failed to find evidence for

**Scheme 1. Structure of 1 and Spectroscopic Features**

**NMR** ($C_6D_6$, 600 MHz)
**$^1$H hydrides**
$\delta$ -6.47 (tdd, $J_{PH}$ = 31, 15, $J_{HH}$ = 6 Hz, 1H)
$\delta$ -8.30 (dtd, $J_{PH}$ = 74, 29, $J_{HH}$ = 6 Hz, 1H)
**$^{31}$P{$^1$H}**
$\delta$ 57.6 (d, $J_{PP}$ = 17 Hz, 2P)
$\delta$ 45.4 (t, $J_{PP}$ = 17 Hz, 1P)
**$^{13}$C{$^1$H}**
$\delta$ 139.4 ($J_{PC}$ = 9.0 Hz, CO)
**IR** $\nu$(CO) 1940 cm$^{-1}$ ($C_6D_6$)
**UV** 325 nm (sh, $\varepsilon$ 9.2 x 10$^3$ M$^{-1}$ cm$^{-1}$, $C_6D_6$)

a further process because of the limitations of the methodology and the techniques available to us at the time: neither the transient absorption nor the TRIR experiments probed the time scale of 0.5−500 ns, and our steady-state NMR experiments were conducted at room temperature and not at low temperature.

The advent of in situ photochemistry at low temperature with NMR detection[16−25] offered a new method of probing reaction mechanisms. In the case of a ruthenium complex related to **1** in which one phosphine has been replaced by an N-heterocyclic carbene, $Ru(H)_2(IEt_2Me_2)(PPh_3)_2(CO)$ ($IEt_2Me_2$ = 1,3-bis(ethyl)-4,5-dimethylimidazol-2-ylidene), we showed that the products are actually consistent with two competing pathways: reductive elimination of $H_2$ and dissociation of $PPh_3$.[26] Loss of $PPh_3$ was revealed by the formation of a cyclometalation product in the absence of other substrates and $Ru(H)_2(IEt_2Me_2)(PPh_3)(CO)(L)$ (L = pyridine, $\eta^2$-$H_2$) in the presence of $H_2$ or pyridine. The combination of this photochemical technique with $p$-hydrogen-induced polarization (PHIP) showed weakly enhanced NMR resonances for the precursor and stronger enhancement for two of its isomers. This effect could be understood by photoinduced reductive elimination of $H_2$ followed by oxidative addition of $p$-$H_2$. Photochemical loss of phosphine competing with loss of $H_2$ was also observed for $Ru(H)_2(PMe_3)_4$.[27] The time scales available and the sensitivity of TRIR spectroscopy have improved greatly since our 1997 study, and there are no longer any gaps in the nanosecond time domain.[28−31]

Recently, we returned to the photochemistry of **1** and observed some unexpected features in its reactivity toward $p$-$H_2$. We found that we could observe PHIP-enhanced hydride resonances if we used a pulsed laser for excitation (at 355 nm) synchronized to the NMR spectrometer under a pressure of $p$-$H_2$.[32] Under these very dilute conditions with single laser shots, there was negligible photodecomposition. Notably, the observed signal enhancement decayed on a millisecond time scale and was only observed with synchronization. This behavior was very different from that of related ruthenium complexes. A paper published in 2017 has repeated these measurements with 308 nm irradiation and a hydrogen pressure of 1 atm. The results are similar, but some photodecomposition has been reported.[33]

In this paper, we report a series of studies of the photochemistry of **1** by NMR and IR methods; the NMR studies were performed using three types of experiments: (a) broad-band ($\lambda$ >290 nm) ex situ irradiation, (b) continuous wave (cw) laser ($\lambda$ 325 nm) in situ irradiation (NMR operating frequency 400 MHz), and (c) pulsed laser ($\lambda$ 355 nm) in situ irradiation (NMR operating frequency 600 MHz). The studies

were conducted at temperatures ranging from 220 to 300 K. The infrared studies include time-resolved IR spectroscopy at room temperature on time scales from nanoseconds to microseconds and FTIR methods at ca. 220 K. They reveal that photodissociation of $PPh_3$ occurs in addition to reductive elimination of $H_2$, leading to substitution products. We show that it is the interplay of these two pathways that limits the use of PHIP methods when they are applied to **1**.

## ■ RESULTS

**Characterization of $Ru(H)_2(CO)(PPh_3)_3$ (1) and Detection of Hyperpolarized 1.** Complex **1** (Scheme 1) has been characterized previously,[15,34] but a summary of its main spectroscopic features is provided in Scheme 1 and a $^1$H NMR spectrum of the key hydride region is illustrated in Figure 1a; a $^{31}$P{$^1$H} NMR spectrum is shown in the Supporting Information.
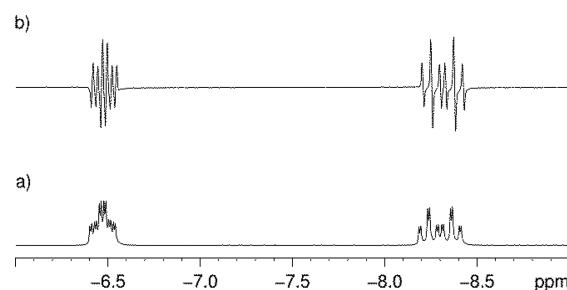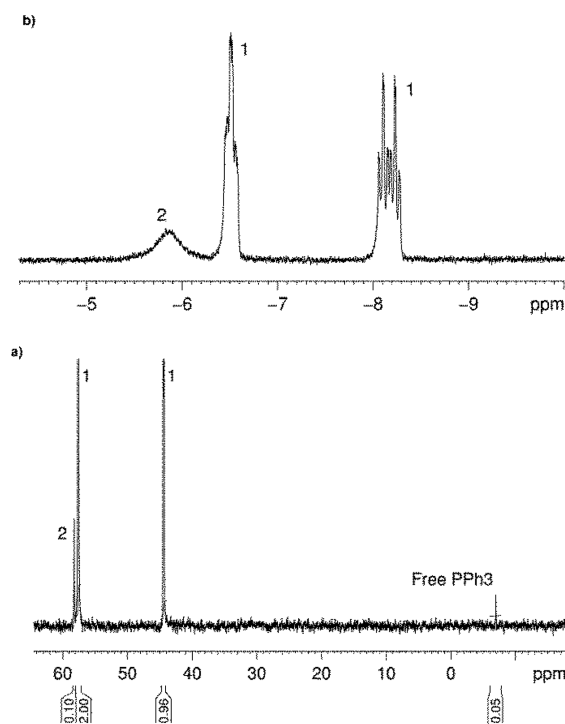


**Figure 1.** Hydride region of two $^1$H NMR spectra of **1** in $C_6D_6$ after (a) 128 scans probing a concentrated solution of **1** and (b) 1 scan of an optically dilute solution after laser-induced incorporation of $p$-$H_2$ yielding hyperpolarized hydride peaks ($\tau$ = 150 $\mu$s).

When an optically dilute solution of **1** is irradiated with a single shot of the pulsed laser (355 nm) in the presence of $p$-$H_2$ (3 bar) and monitored through the response from a single, synchronized rf pulse that takes place up to 5 ms after laser irradiation, enhanced hydride signals at $\delta$ −6.47 and −8.30 are observed (Figure 1b). In this spectrum, $J_{HH}$ corresponds to the peak separation of the antiphase features, while the other splittings arise from coupling to $^{31}$P nuclei[32] (the corresponding $^1$H{$^{31}$P} spectrum is shown in the Supporting Information). Similar hyperpolarization is observed on irradiation at 220 K. This result demonstrates that $p$-$H_2$ has been incorporated into **1**. Formation of hyperpolarized **1** can be understood by reductive elimination of $H_2$ upon 355 nm irradiation yielding $[Ru(CO)(PPh_3)_3]$, which recombines with $p$-$H_2$ by oxidative addition. The readdition of $H_2$ to $[Ru(CO)(PPh_3)_3]$ is known to be fast under these conditions (the time constant for recombination under 3 atm of $H_2$ is 1.4 $\mu$s), precluding the detection of any transient species.

**NMR Studies of the Photochemistry of 1.** *Formation of $Ru(H)_2(\eta^2$-$H_2)(CO)(PPh_3)_2$ (2).* In contrast to the measurements described above, the steady-state photolysis of an optically dilute solution of **1** under a $p$-$H_2$ atmosphere at 295 K in benzene-$d_6$ or toluene-$d_8$ undertaken either ex situ ($\lambda$ >290 nm) or in situ with a laser ($\lambda$ 325 nm, cw) resulted in no change in the observed NMR spectra of these solutions and PHIP was no longer observed in the hydride resonances of **1**. Notably, a very intense peak for $o$-$H_2$ was visible before irradiation was initiated, indicating consumption of $p$-$H_2$ via a thermal route.

When the in situ irradiation process with $p$-$H_2$ was repeated at 223 K (toluene-$d_8$), there was still no PHIP enhancement of **1** upon photolysis (2 min, $\lambda$ 325 nm). However, a new broad resonance (fwhm ca. 63 Hz at 400 MHz) was observed at $\delta$ −5.82 in the $^1H$ NMR spectrum along with new signals in the aromatic region indicating productive photochemistry and the formation of the new species **2** (Figure 2a).



**Figure 2.** NMR spectra after the photolysis of **1** under $p$-$H_2$ in toluene-$d_8$ at 220 K: (a) $^{31}P\{^1H\}$ NMR spectrum showing the formation of **2** and free PPh$_3$; (b) hydride region of the $^1H$ spectrum displaying signals for **1** and a broad resonance for **2**.

The $^{31}P\{^1H\}$ NMR spectrum now displayed two new singlets at $\delta$ −6.0 and 59.4 in addition to the resonances of **1**. The new $^{31}P\{^1H\}$ peak resonating at $\delta$ −6.0 was identified as free PPh$_3$, and an experiment with inverse-gated decoupling (quantitative phosphorus) showed that the integration ratio of the unknown peak to the free PPh$_3$ is 2:1, suggesting that **2** contains two equivalent PPh$_3$ ligands (Figure 2b). Further cooling to 193 K resulted in no change in these NMR features; however, warming to 295 K led to the disappearance of these signals and re-formation of **1**. Complex **2** could also be generated at low temperatures with pulsed laser irradiation ($\lambda$ 355 nm, 48 laser shots, 10 Hz repetition rate). On the basis of these results, we assign **2** as the dihydrogen complex Ru(H)$_2$($\eta^2$-H$_2$)(CO)(PPh$_3$)$_2$ formed by photochemically induced PPh$_3$ loss from **1** and coordination of H$_2$ (Scheme 2). Upon cooling to 193 K the associated NMR spectra of **2** show minimal change. Moreover, when a $^1H\{^{31}P\}$ NMR spectrum was recorded at 220 K using a broad-band decoupling sequence, the peak for **2** remained unaltered whereas the resonances for **1** simplified to doublets retaining only a $J_{HH}$ value of 6 Hz between the two hydrides. These observations are fully consistent with rapid exchange between hydride and dihydrogen ligands in conjunction with quick relaxation and the averaging of hydride−phosphorus couplings to a small and hence invisible value. The exchange is likely to occur by the $\sigma$-CAM mechanism,[35] as has been shown

**Scheme 2. Competing Photochemistry of 1 under H$_2$ Atmosphere**
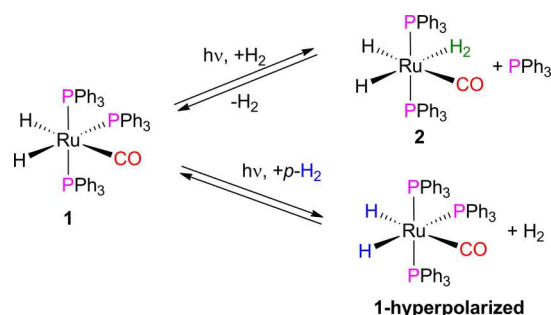


in detail by Crabtree.[36] Furthermore, the disappearance of **2** upon warming is consistent with the well-known lability of dihydrogen as a two-electron-donor ligand.[37] Complex **2** is an analogue of Ru(H)$_2$($\eta^2$-H$_2$)(PPh$_3$)$_3$ that is formed from Ru(H)$_2$(PPh$_3$)$_4$ thermally and is also closely related to [Ru(IPr)$_2$(CO)($\eta^2$-H$_2$)H]BArF$_4$ (IPr = 1,3-bis(2,6-diisopropylphenyl)imidazol-2-ylidene).[38−40] Comparisons may also be made to Ru and Ir complexes studied with partial deuteration.[41,42]

In order to confirm the presence of a dihydrogen ligand in **2**, data for $T_1$ were recorded at 400 MHz between 212 and 242 K for the resonance at $\delta$ −5.82. The value of $T_1$(min) for **2** proved to be 35 $\pm$ 2 ms at ca. 225 K, whereas the corresponding value of $T_1$ for the hydride resonances of **1** was much longer (390 ms at 298 K). This is consistent with a dihydrogen arrangement, as such ligands are known to relax much more quickly than their hydride analogues.[37,43] Further analysis of the $T_1$ values is given in the Supporting Information.

We have already shown that PHIP was observed for the hydride resonances of **1** when a solution of **1** (C$_6$D$_6$) under $p$-H$_2$ (~4 bar) was irradiated at 298 K with a pulsed laser (355 nm) synchronized to the spectrometer.[32] However, if this sample was irradiated with multiple laser shots (4 sets of 32 laser shots, 10 Hz repetition rate, 1 NMR scan), **2** was detected, although its signal disappeared after the first NMR scan due to its low stability. As complex **2** disappeared, the signals for **1** and a new hydride resonance started to grow in a thermal reaction. This new product signal appears at $\delta$ −6.34, as a triplet with $J$ = 23 Hz, that connects to a single $^{31}P\{^1H\}$ resonance at $\delta$ 57.1 and simplifies into a singlet upon $^{31}P$ decoupling; it is assigned to the known Ru(H)$_2$(PPh$_3$)$_2$(CO)$_2$.[44,45]

Additional evidence for formation of **2** was obtained by photolysis of **1** under a D$_2$ atmosphere at 298 K using either a pulsed or continuous laser. Depletion of the hydride signal for **1** occurred during photolysis along with the appearance of peaks for H$_2$ ($\delta$ 4.46 in C$_6$D$_6$, s) and HD ($\delta$ 4.41 in C$_6$D$_6$, t, $J_{HD}$ = 43 Hz). There was also evidence of partial deuteration of **1** through broadening of the hydride resonances. Direct reductive elimination accounts for the formation of H$_2$. HD is logically formed through loss of PPh$_3$ and initial $\eta^2$ coordination of D$_2$ to form the deuterium analogue of **2** followed by intramolecular exchange with the hydride ligands to yield Ru(H)(D)(HD)(CO)(PPh$_3$)$_2$ and ultimately HD. Complex **1-d$_2$** was generated by a sequence of three cycles of photolysis of **1** under D$_2$ (3 atm), followed by replacement of the atmosphere by fresh D$_2$ and further photolysis. At this stage, no HD or hydride resonances for **1** could be detected. Photoreaction (325 nm) of the preformed **1-d$_2$** with H$_2$ at 223 K was then followed by $^1H$ NMR and, as expected, the hydride signals of both **1** and **2**

were seen. Although this sample should contain partially deuterated **2**, no $J_{HD}$ splitting was observed, even at 193 K. The lack of a visible HD splitting is consistent with rapid exchange between the hydride and dihydrogen ligands.[37]

Although the two hydride ligand signals of **1** are distinct at room temperature, heteronuclear NOESY experiments have previously demonstrated that **1** undergoes intramolecular ligand exchange at 335 K where the two hydrides exchange with each other as well as with the inequivalent phosphines.[46] The exchange was postulated to occur via a trigonal twist mechanism, but alternative mechanisms involving dihydrogen isomers are also possible (see Discussion). We undertook a series of 1D EXSY experiments to probe for the thermal exchange of **1** with free $H_2$ or free PPh$_3$. The two hydride peaks and free hydrogen peak were monitored at mixing times between 50 and 800 ms in C$_6$D$_6$ solution. As expected, slow intramolecular exchange between the two hydride resonances was observed at room temperature and faster exchange at 333 K as previously reported,[46] but no exchange with free $H_2$ was detected up to 333 K, demonstrating that no thermal $H_2$ elimination occurs on the EXSY time scale of ca. 1 s (see the Supporting Information). In similar experiments, exchange between free PPh$_3$ and the phosphine ligands was monitored at 333 K (see the Supporting Information). Once more, no intermolecular exchange was observed, in agreement with the literature.[46]

The photoreactions of **1** under $H_2$ provide evidence for $H_2$ reductive elimination and readdition through PHIP of **1**; evidence for competing PPh$_3$ dissociation is seen via the observation of **2** and the formation of HD on photolysis under $D_2$.

*Formation of Ru(H)$_2$(AsPh$_3$)(CO)(PPh$_3$)$_2$ (3).* In order to further probe the phosphine loss pathway, a sample of **1** (C$_6$D$_6$) was prepared under p-$H_2$ (~4 bar) in the presence of a 10-fold excess of AsPh$_3$. A $^1$H{$^{31}$P} NMR spectrum measured prior to photolysis revealed slight conversion of **1** into the new species **3** with two very weak hydride resonances at $\delta$ −6.28 and −9.46 ($J_{HH}$ = 6 Hz) and a new singlet in the $^{31}$P{$^1$H} spectrum at $\delta$ 58. When the sample was exposed to a single laser shot at 295 K, the hydride resonances of both **1** and **3** became PHIP-enhanced (Figure 3). The intensities of the new product peaks were also found to increase on irradiation with more laser shots. These peaks are split into triplets of antiphase doublets, in an overall 1:1 intensity ratio, in the $^1$H NMR
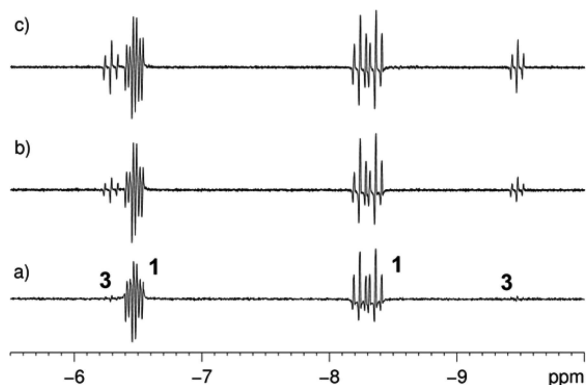


**Figure 3.** Hydride region of a series of $^1$H NMR spectra of a solution of **1** in C$_6$D$_6$ in the presence of a 10-fold excess of AsPh$_3$ under p-$H_2$ at room temperature showing hyperpolarized signals for **1** and **3** after (a) 1 laser shot, (b) 2 laser shots, and (c) 4 laser shots.

spectrum and simplify into antiphase doublets upon $^{31}$P decoupling. The triplet splitting is due to coupling to two equivalent $^{31}$P nuclei that lie *cis* to the hydrides ($\delta$ −6.28, $J_{PH}$ = 30 Hz; $\delta$ −9.46, $J_{PH}$ = 26 Hz). We therefore assign **3** to Ru(H)$_2$(AsPh$_3$)(CO)(PPh$_3$)$_2$, formed by PPh$_3$ loss and AsPh$_3$ coordination, with the geometry shown in Scheme 3. Free PPh$_3$

**Scheme 3. Photochemistry of 1 in the Presence of Excess AsPh$_3$ and p-H$_2$**
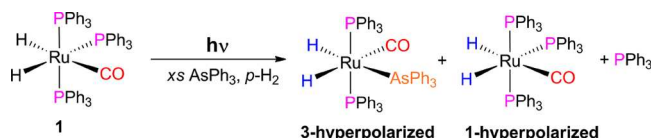


was detected in the $^{31}$P{$^1$H} spectrum, as expected. Some thermal loss of PPh$_3$ occurs, as is evident from the presence of a small amount of **3** before irradiation. Additionally, these observations also confirm that photolysis causes PPh$_3$ loss along with $H_2$ reductive elimination. Complex **3** is relatively stable and can still be detected at room temperature after the p-$H_2$ response has decayed.

*Formation of Ru(H)$_2$(CO)(PPh$_3$)$_2$(pyridine).* An analogous reaction was then undertaken where AsPh$_3$ was replaced with pyridine. The thermal reaction of **1** with pyridine under p-$H_2$ (4 bar) at 298 K was first monitored in toluene-d$_8$ with added pyridine (10 $\mu$L). No reaction was observed by conventional NMR spectroscopy at 295 K; notably, the presence of pyridine suppressed the conversion of p-$H_2$ to o-$H_2$ that had been observed in the absence of pyridine. However, when this process was repeated using the high-sensitivity Only Pp-hydrogen SpectroscopY (OPSY)[47] approach, two weak hydride resonances were observed that we assign to the complex Ru(H)$_2$(CO)(PPh$_3$)$_2$(pyridine) (**4-CN**). (We label the isomers of **4** according to the ligands that lie *trans* to the mutually *cis* hydride ligands. Thus, **4-CN** indicates that the *cis* hydride ligands are *trans* to C and N; see below.) Conversion to this product improved on increasing the temperature to 345 K, confirming a thermal route to its formation. The same product could be generated more efficiently by photochemical reaction in neat pyridine; after 3 h irradiation ($\lambda$ >290 nm, 295 K), 80% of the starting material **1** was converted to **4-CN** along with some minor byproducts (see later).

The hydride region of the $^1$H NMR spectrum, measured without hyperpolarization, shows two major resonances for **4-CN** as a triplet of doublets at $\delta$ −4.59 ($J_{PH}$ = 27 Hz, $J_{HH}$ = 6.5 Hz) and $\delta$ −14.32 ($J_{PH}$ = 23 Hz, $J_{HH}$ = 6.5 Hz) in a 1:1 ratio. These signals simplify into doublets when $^{31}$P is decoupled. The corresponding $^{31}$P{$^1$H} NMR spectrum displayed a singlet at $\delta$ 65.4 for the main product. On the basis of these results we assign **4-CN** to Ru(H)$_2$(CO)(PPh$_3$)$_2$(NC$_5$H$_5$), an analogue of **3**, with mutually *trans* PPh$_3$ groups formed by photochemical PPh$_3$ loss and reaction with pyridine. The hydride resonance at $\delta$ −14.32 displayed a chemical shift characteristic of a hydride *trans* to nitrogen,[48] while the remaining hydride is assigned as *trans* to CO; free PPh$_3$ was also detected in the $^{31}$P{$^1$H} spectrum. Attempts to isolate **4-CN** were unsuccessful due to the lability of the pyridine ligand; when the sample was pumped to dryness and redissolved in benzene, **1** was regenerated almost quantitatively (see the Supporting Information). When this reaction was repeated with a 10-fold excess of C$_5$D$_5$N in benzene, the same product distribution was observed.

Irradiation of **1** in $C_6D_6$ under $p$-$H_2$ (4 bar) in the presence of a 10-fold excess of pyridine-$d_5$ with the pulsed laser at 295 K led to the detection of strongly hyperpolarized **1** (Figure 4a)
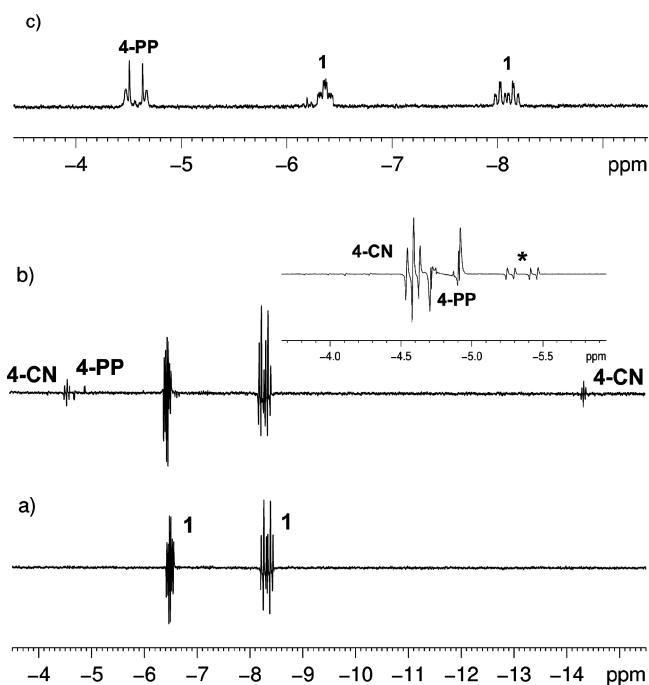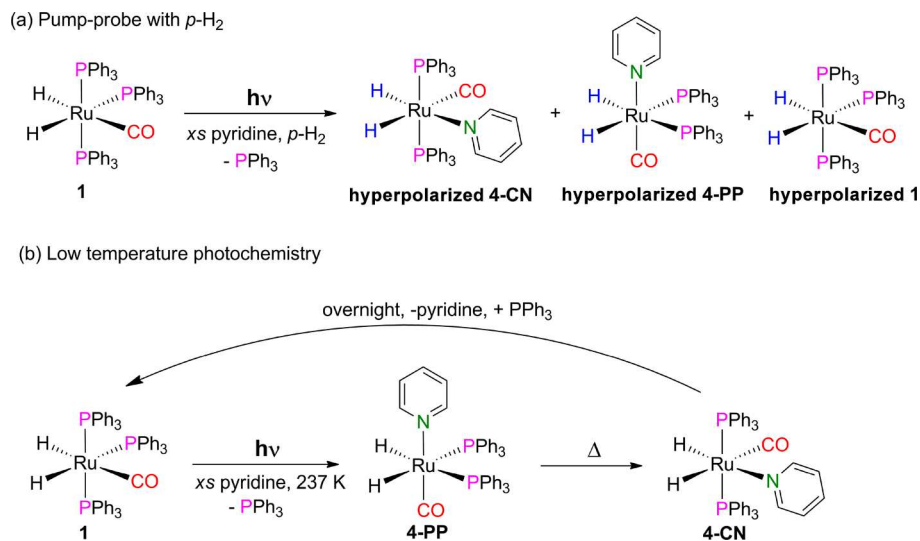


**Figure 4.** Hydride region of a series of $^1$H spectra of **1** under $p$-$H_2$ in the presence of excess $C_5D_5N$ at room temperature (a) after a single laser shot in $C_6D_6$ solution showing hyperpolarized **1** and (b) after two consecutive laser shots in $C_6D_6$ solution showing the formation of hyperpolarized **4-PP** and **4-CN**. The inset in (b) shows an expansion of the hydride peak for hyperpolarized **4-PP** (the inset spectrum was acquired with 4 laser shots, and the doublet of antiphase doublets marked by an asterisk is due to another isomer, **4-NP**; see below). (c) Spectrum acquired at 237 K in toluene-$d_8$ without hyperpolarization, showing signals for the primary photochemical product **4-PP** with a typical AA′XX′ appearance (the change in chemical shift is due to use of a different solvent).

after a single laser shot with a single NMR scan.[32] When the laser was allowed to fire two shots consecutively (10 Hz repetition rate), PHIP-enhanced resonances of **4-CN** also became visible after one NMR scan, observed as triplets of antiphase doublets in the $^1$H NMR spectrum. A weakly hyperpolarized resonance at $\delta$ −4.82 with a shape that indicates a product with an AA′XX′ spin system was also observed (Figure 4b). We assign it to **4-PP**, an isomer of **4-CN** with a square-planar $Ru(H)_2(PPh_3)_2$ skeleton where the two hydrides and two phosphines are mutually *cis* (Scheme 4a). In this situation, the two hydrides are chemically equivalent but magnetically inequivalent because of *cis* and *trans* phosphorus couplings, which satisfies the symmetry-breaking conditions needed to detect PHIP. The $^{31}$P resonance of **4-PP** was found at $\delta$ 47.8.

The identities of **4-CN** and **4-PP** were confirmed by in situ irradiation of a $C_6D_6$ solution of **1** in the presence of a 10-fold excess of $^{15}N$-pyridine under $p$-$H_2$ pressure with the pulsed laser. $^1$H−$^{15}$N HMQC spectroscopy showed a cross peak between the hydride peak at $\delta$ −14.32 for complex **4-CN** and a resonance at $\delta$ 270.4 in the $^{15}$N spectrum which now exhibits a *trans* $^{15}$N coupling of $J_{NH}$ = 12 Hz (see the Supporting Information). A cross peak was also observed between the hydride resonance for complex **4-PP** and a signal in the $^{15}$N NMR spectrum at $\delta$ 256.3, indicating a small *cis* $J_{NH}$ coupling (<2 Hz).

The irradiation of a solution of **1** in $C_6D_6$ in the presence of a 10-fold excess of $C_5D_5N$ under $p$-$H_2$ pressure at room temperature (Figure 5a) with 32 pulsed laser shots (355 nm, 10 Hz repetition rate) resulted in almost quantitative conversion to **4-CN** (Figure 5b). Given that we are only irradiating a small sample cross section but monitoring across the whole sample, we can confirm that diffusional mixing is rapid on this time scale in order to allow for the quantitative conversion. When this sample was shaken to refresh the dissolved $p$-$H_2$ to test thermal exchange between free $H_2$ and the hydrides of **4-CN**, PHIP was detected on the hydride resonances (Figure 5c), leading to the conclusion that the hydride ligands of the pyridine complex **4-CN** exchange thermally with free $H_2$ at room temperature. These

**Scheme 4. Photoreactions of 1 with Pyridine; (a) Pump-Probe Photochemistry of 1 under $p$-$H_2$ Atmosphere; (b) Low-Temperature Photochemistry**
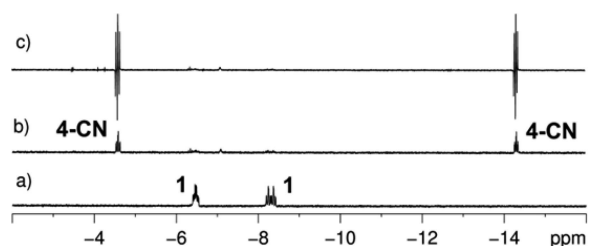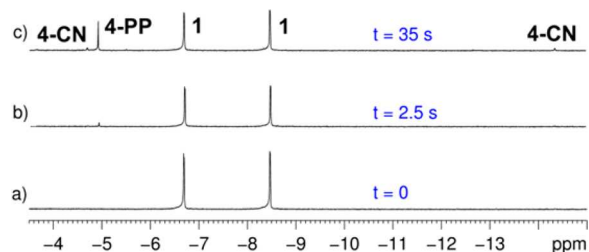
**Figure 5.** Hydride region of a series of ^{1}H NMR spectra of a solution of **1** in $C_6D_6$ in the presence of a 10-fold excess of $C_5D_5N$ under $H_2$ pressure at room temperature: (a) hydride resonances of **1** before laser irradiation; (b) resonances after 32 laser shots at 355 nm showing mainly **4-CN**; (c) resonances of the same sample after being shaken with $p$-$H_2$ that displays PHIP of **4-CN**.

observations contrast with the behavior of **1**, for which no direct thermal exchange with free $H_2$ was observed at room temperature. When the same solution of **4-CN** is left overnight and checked again by NMR, quantitative regeneration of the starting complex **1** is observed, highlighting the lability of the pyridine ligand, which is slowly displaced by the stoichiometric amount of PPh$_3$ present in solution after photosubstitution.

The photoreaction of **1** with pyridine (10 μL) under $p$-$H_2$ was also studied with cw laser irradiation (325 nm) at 223 K in toluene-$d_8$. Following photolysis (2 min), hyperpolarized signals were observed for **4-CN** and **4-PP** but not for **1**. (Note that no hyperpolarization of **1** is observed unless the pulsed laser is used and synchronized with the rf pulse of the spectrometer.) There was no evidence for the formation of **2** in these spectra, but the persistence of hyperpolarization after the photolysis source has been switched off confirms that **4-CN** and **4-PP** continue to undergo rapid thermal hydride ligand exchange with $p$-$H_2$ as demonstrated above.

In order to probe the isomerization of **4-CN** and **4-PP**, in situ photolysis of **1** in neat $C_5D_5N$ was conducted at 237 K without a $H_2$ atmosphere. After 24 laser shots, 2.5% conversion was observed, with the initial ratio of **4-PP** to **4-CN** being 2:1. Further photolysis increased the overall conversion level without a change in the ratio of **4-PP** to **4-CN** (Figure 6).



**Figure 6.** Hydride region of a series of [1]H{[31]P} spectra of a solution of **1** in neat $C_5D_5N$ at 237 K: (a) starting solution at photolysis time 0; (b) solution after 2.5 s photolysis at 355 nm; (c) solution after 35 s photolysis.

The proportion of **4-CN** increased, however, with an increase in temperature, suggesting thermal equilibration between the two isomers (Figure 7). When the solution was warmed to room temperature, **4-PP** converted to **4-CN** quantitatively. Totally analogous behavior was found when the same experiment was repeated under a $H_2$ atmosphere (4 bar). Similarly, no changes in behavior were observed when the reaction was run in toluene-$d_8$ with a 10-fold excess of pyridine.
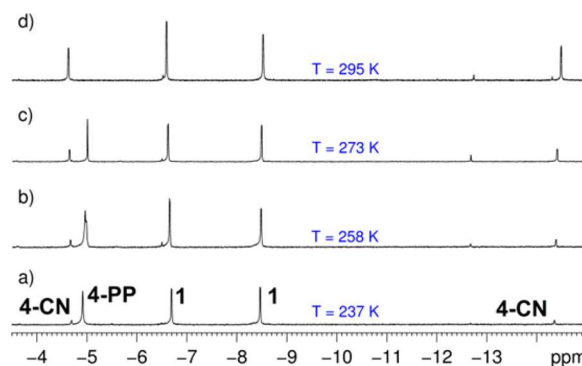


**Figure 7.** Hydride region of a series of [1]H{[31]P} spectra of a solution of **1** in neat $C_5D_5N$ after 140 s of photolysis showing equilibration between **4-PP** and **4-CN** with increasing temperature: (a) $T$ = 237 K; (b) $T$ = 258 K; (c) $T$ = 273 K; (d) $T$ = 295 K.

These experiments lead to the surprising conclusion that **4-PP** is the first product of this reaction to be formed at low temperature that is stable on an NMR time scale: i.e., the primary photoproduct (Scheme 4b).

We then used the PHIP effect to search for the formation of minor products in this reaction. When a sample of **1** under $p$-$H_2$ in $C_6D_6$ with a 10-fold excess of pyridine was exposed to multiple shots (up to 8) of the pulsed laser (355 nm), two new hyperpolarized minor species appeared in addition to those of **4-CN** and **4-PP** (Figure 8). Furthermore, under these higher
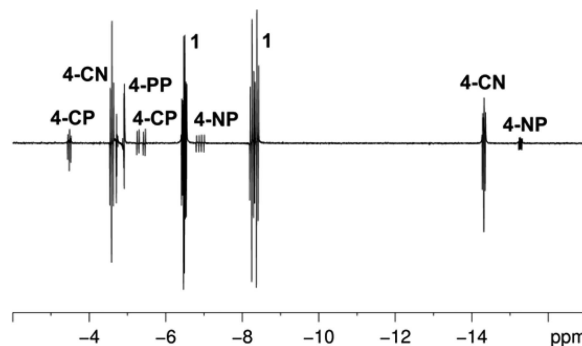


**Figure 8.** Hydride region of the hyperpolarized ^{1}H NMR spectrum of a $C_6D_6$ solution of **1** under $p$-$H_2$ in the presence of excess $C_5D_5N$. The solution was monitored after 8 laser shots.

signal to noise conditions hyperpolarization was clearly visible in the ortho aromatic protons of **4-PP** and the ^{31}P resonance of this complex at $\delta$ 47.8 (see the Supporting Information). Analogous behavior has been observed before for a complex with chemically equivalent but magnetically inequivalent hydrides.[32] The hydride resonances for the first of these species, complex **4-NP**, appear at $\delta$ −6.91 and −15.28 (Scheme 5). The hydride at $\delta$ −6.91 was assigned to lie *trans* to a PPh$_3$ group because of the large $J_{PH}$ coupling (79 Hz; *cis* $J_{PH}$ was measured as 40 Hz). The other hydride ligand of **4-NP** was detected by photochemical hyperpolarized COSY and assigned to lie *trans* to pyridine ($J_{PH}$ = 16, 30 Hz, see the Supporting Information for COSY). The second product, **4-CP**, exhibits a much weaker pair of hydride ligand signals whose chemical shifts and coupling constants ($\delta$ −3.47, $J_{PH}$ = 23, 30 Hz; $\delta$ −5.35, $J_{PH}$ = 32, 98 Hz) indicated that one hydride is *trans* to CO and the other *trans* to PPh$_3$. With ^{15}N-labeled pyridine, a very weak cross peak between the hydride peak at $\delta$ −15.28 of

**Scheme 5. Structures of the Minor Photolysis Products with Added Pyridine**
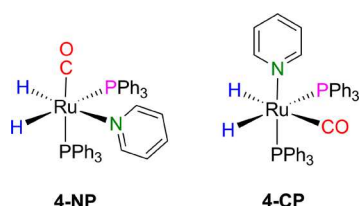


complex **4-NP** and a signal in the $^{15}$N NMR spectrum at $\delta$ 266.2 was also detected ($J_{NH}$ = 14 Hz), confirming that the pyridine lies *trans* to the hydride, as indicated by the characteristic chemical shift. No $^{15}$N$-^1$H cross peaks were observed for **4-CP**. A change of the solvent to neat pyridine did not provide additional information.

In order to quantify the ratio of H$_2$ reductive elimination to PPh$_3$ loss, a sample of **1** was irradiated (355 nm) with the same concentration of D$_2$ and pyridine-$d_5$ (both 0.012 M, 10-fold excess) at 300 K. Under these conditions, H$_2$ loss is followed by D$_2$ oxidative addition to form **1-$d_2$**; loss of PPh$_3$ leads to conversion to the pyridine complex **4-CN**. Pentafluoroanisole was used as an internal standard after ensuring that the compound was inert to it under these reaction conditions. $^1$H NMR spectra were acquired at different photolysis time intervals; the reaction was taken to 50% conversion. The overall quantity of **1** and **1-$d_2$** was measured by integration of the ortho protons (12 H; $\delta$ 7.46) for the axial phenyl rings of **1** that are well resolved. The integration of the hydride peak of **1** reported on the amount of **1** that remained undeuterated. The ortho protons (12 H) of **4-CN** ($\delta$ 7.94) quantified the production of **4-CN**. Because of thermal exchange with D$_2$ (see above), the hydride resonances for complex **4-CN** were not detected. This experiment established that, at 50% conversion of **1**, H$_2$ reductive elimination accounts for ≤40% of the photochemical reactivity while PPh$_3$ loss takes place with 60% probability. We were concerned that under these conditions formation of **2-$d_2$** could compete with formation of **4-CN** following loss of PPh$_3$. We therefore repeated the experiment under exactly the same conditions but with a large excess of pyridine with respect to D$_2$ in order to turn formation of **2-$d_2$** into an uncompetitive route. Under these conditions, the ratio of PPh$_3$ loss to H$_2$ reductive elimination products was 52:48. These results indicate approximately the same quantum yields for the two photochemical processes.

We have previously shown that it is possible to probe the hydride signal intensities under hyperpolarization conditions in a series of NMR measurements recorded as a function of the delay, $\tau$, between the laser irradiation step and the rf pulse. When an optically dilute solution of **1** in C$_6$D$_6$ is used and the appropriate laser energy applied, there is no decomposition of the sample due to photolysis; this allows the same solution to be used multiple times. The response is expected to oscillate at the frequency difference between the two coupled hydride resonances ($\Delta\nu$ for **4-CN** in C$_6$D$_6$ 9.75 ppm = 5851 Hz).[32,49] The evolution of the PHIP-enhanced NMR signals for **4-CN** was investigated in this way. A C$_6$D$_6$ solution of **1** in the presence of excess pyridine under $p$-H$_2$ (4 bar) was therefore irradiated with the pulsed laser (355 nm). The resonances of **1** oscillate in intensity as reported before. Analogous coherent oscillations in intensity were found for the hydride resonances of **4-CN** at a frequency of 5850 ± 5 Hz. Figure 9 illustrates the

oscillation in the form of a 2D spectrum Fourier-transformed with respect to the pump−probe delay, $\tau$.
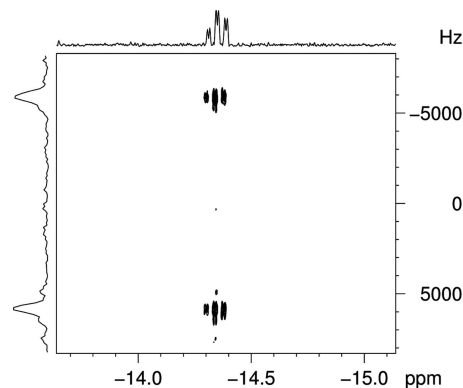


**Figure 9.** 2D $^1$H pump−probe NMR spectrum of a C$_6$D$_6$ solution of **4-CN** where the vertical dimension corresponds to evolution frequency encoded by $\tau$. Measurements were made with four laser pulses followed at delay $\tau$ by a single NMR pulse. Hydrides $\Delta\nu$ in C$_6$D$_6$ 9.75 ppm = 5851 Hz, oscillation frequency 5850 ± 5 Hz.

The NMR results demonstrate clearly that two competing pathways occur during the photochemistry of complex **1**. One photochemical process is H$_2$ reductive elimination, as demonstrated by the observation of PHIP in the associated hydride peaks after irradiation under a $p$-H$_2$ atmosphere and incorporation of deuterium if photolysis is carried out under a deuterium pressure. In situ photolysis at low temperature led to the discovery of a competing photochemical pathway involving PPh$_3$ loss, first identified through the formation of the dihydrogen complex **2**. Subsequently, the triphenylarsine complex **3** and the pyridine complexes **4-CN** and **4-PP** were formed without the need for low temperatures. We determined that quantum yields for H$_2$ reductive elimination and PPh$_3$ loss at 300 K are approximately equal. The use of $p$-H$_2$ is critical to revealing some of these species. However, the formation of the dihydrogen complex **2** causes $p$-H$_2$ relaxation, but this conversion can be suppressed by addition of other ligands such as pyridine. We observed no Ru(0) products at either room temperature or low temperature. We therefore wished to know if evidence from TRIR spectroscopy is compatible with these conclusions.

**IR Studies.** In the earlier experiments, the transient [Ru(PPh$_3$)$_3$(CO)] was detected by both time-resolved UV− vis and IR spectroscopy of **1** ($\lambda_{max}$ 380 nm, $\nu$(CO) 1845 cm$^{-1}$) and found to react with H$_2$ to regenerate **1** on a microsecond time scale ($k_2$ = (8.4 ± 0.4) × 10$^7$ dm$^3$ mol$^{-1}$ s$^{-1}$). The unsaturated species [Ru(PPh$_3$)$_3$(CO)] was found to be formed within 6 ps by ultrafast TRIR, indicating that reductive elimination of H$_2$ also takes place on this time scale.[15] Our new results suggested that it should also be possible to detect PPh$_3$ loss by TRIR spectroscopy. We have therefore undertaken new TRIR experiments with modern equipment with higher sensitivity and nanosecond time resolution. We first report investigations of the photochemistry of **1** by low-temperature FTIR spectroscopy.

*Photolysis of **1** Monitored by FTIR Spectroscopy.* Figure 10a shows the IR difference spectra obtained following irradiation of a solution of **1** in toluene-$d_8$ at 220 K under Ar. The parent $\nu$(CO) band at 1937 cm$^{-1}$ is bleached, and a new band at 1980 cm$^{-1}$ is formed. The band at 1980 cm$^{-1}$ can
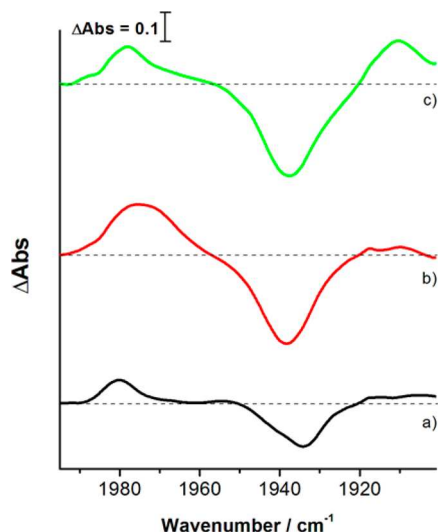
**Figure 10.** Difference spectra of **1** after photolysis at 220 K in toluene-$d_8$ (a) under argon, (b) under hydrogen (ca. 1 atm), and (c) with added pyridine in toluene-$d_8$ (0.1 mL in 5.0 mL) under argon. The $\Delta$Absorbance values have been normalized.
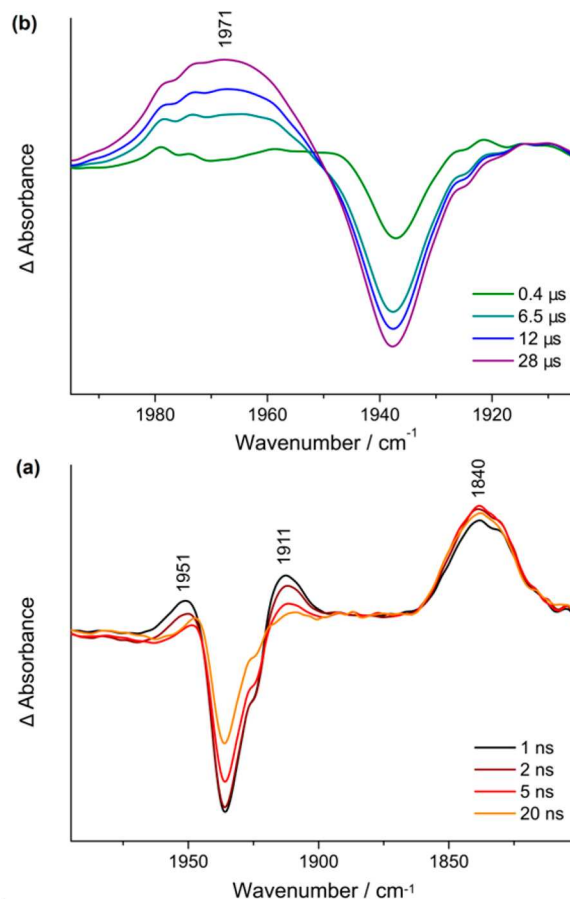


**Figure 11.** TRIR difference spectra obtained in the ranges (a) 1–20 ns and 1900–2000 cm$^{-1}$ and (b) 0.4–28 $\mu$s and 1800–2000 cm$^{-1}$, after a 355 nm laser flash of a solution of **1** in C$_6$D$_6$ under an atmosphere of argon.

be assigned to a dimeric product, as was proposed in the previous TRIR studies.[15]

A similar experiment, performed under H$_2$ (1 atm), led to bleaching of the parent band and the production of a broad band at ca. 1975 cm$^{-1}$ (Figure 10b). These spectra were fitted using a multi-Lorentzian function, indicating the presence of two overlapping bands at ca. 1980 and 1971 cm$^{-1}$. The solution was warmed to 240 K, and FTIR spectra were acquired every 3 min. The band at 1971 cm$^{-1}$ decayed much more quickly than the 1980 cm$^{-1}$ band, providing further support for the presence of two bands. The band at 1971 cm$^{-1}$ can be assigned to the hydride dihydrogen species **2**, which arises from phosphine loss and reaction of the [Ru(PPh$_3$)$_2$(CO)(H)$_2$] fragment with H$_2$ in agreement with the result from NMR spectroscopy.

The photolysis of **1** at 220 K was carried out in the presence of added pyridine in toluene under Ar, and again the dimer band was observed together with a new band at 1911 cm$^{-1}$ (Figure 10c). We also carried out a similar experiment at room temperature in benzene with added pyridine-$d_5$ and observed the product at 1921 cm$^{-1}$ (see the Supporting Information). We assign the band at 1921 cm$^{-1}$ to **4-CN** and the band at 1911 cm$^{-1}$ observed at 220 K to **4-PP**, on the basis of the isomer distribution observed by NMR spectroscopy.

*TRIR Spectroscopy.* Earlier TRIR studies were conducted in C$_6$D$_6$ at room temperature and showed that H$_2$ elimination from **1** ($\nu$(CO) 1940 cm$^{-1}$) formed the 16e$^-$ Ru(0) species [Ru(CO)(PPh$_3$)$_3$] with a $\nu$(CO) band at 1840 cm$^{-1}$.[15] These results were obtained covering a time window of 1–1000 $\mu$s employing a lower resolution instrument based on a CO laser.[15] We have repeated these measurements using more sensitive instrumentation with faster time resolution. All of the IR experiments were carried out in optically dilute solutions of **1** in C$_6$D$_6$ for consistency with the NMR experiments.

*TRIR of 1 under an Ar Atmosphere in C$_6$D$_6$.* Figure 11 shows the TRIR difference spectra at 298 K of **1** in C$_6$D$_6$ obtained at 1 ns (a) and 23 $\mu$s (b) following irradiation at 355 nm. The TRIR spectrum obtained after 1 ns shows bleaching of the parent band and a product band at 1840 cm$^{-1}$ (not shown in Figure 11), which was observed in the previous TRIR

experiments[15] and can be assigned to the Ru(0) species [Ru(PPh$_3$)$_3$(CO)] arising from H$_2$ reductive elimination. Two new bands are also produced at ca. 1951 and 1911 cm$^{-1}$, which were not observed in the previous TRIR measurements. The TRIR spectrum obtained 28 $\mu$s after the flash shows that these two bands have decayed and a new absorption is formed due to the dimeric product at 1971 cm$^{-1}$. The bands at 1951 and 1911 cm$^{-1}$ are tentatively assigned to two different isomers of [Ru(PPh$_3$)$_2$(CO)H$_2$] produced by PPh$_3$ loss. These bands decay with two components, a fast component (1.7 ns) that approximately matches rapid re-formation of the parent (ca. 4 ns, Figure 12a,b) and a slower decay (ca. 10 $\mu$s, Figure 12c,d) which is similar to the formation of the dimer band and the further bleaching of the parent. The precise nature of the fast component is not known but could be due to in-cage recombination of photoejected PPh$_3$. The slower kinetics show further bleaching of **1** as the dimer band forms at 1971 cm$^{-1}$. This is consistent with formation of the dimer by reaction of the fragment [Ru(PPh$_3$)$_2$(CO)H$_2$] with the parent **1** (Figure 12c,d).

*TRIR of 1 under H$_2$ in C$_6$D$_6$.* Irradiation of a solution of **1** in the presence of H$_2$ (1 atm) displays, at early time (Figure 13a), a negative band for **1** and new product bands to both higher and lower frequency of the parent. In agreement with the previous results, the formation of [Ru(PPh$_3$)$_3$(CO)] at 1840 cm$^{-1}$ is also observed within the time resolution of 0.5 ns; the transient [Ru(PPh$_3$)$_3$(CO)] was stable up to 28 ns. A product
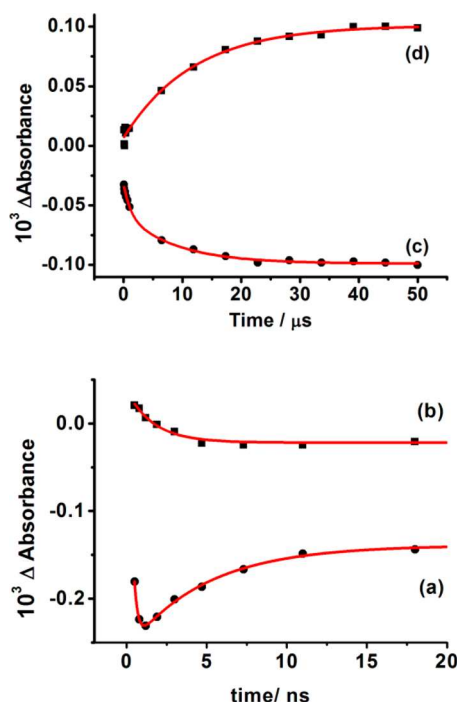
**Figure 12.** Kinetic plots observed after photolysis of **1** under Ar (plots (a) and (b) on a nanosecond time scale and plots (c) and (d) on a microsecond time scale): (a) 1939 cm$^{-1}$ assigned to **1** which shows a rapid increase, followed by a bleach recovery, $\tau$ = 4.8 ± 0.4 ns; (b) 1951 cm$^{-1}$, $\tau$ = 1.7 ± 0.4 ns; (c) 1938 cm$^{-1}$ assigned to **1**, $\tau_1$ = 1.1 ± 0.4 $\mu$s, $\tau_2$ = 9 ± 2 $\mu$s; (d) 1970 cm$^{-1}$ assigned to the dimeric species, $\tau$ = 12 ± 2 $\mu$s. $\Delta$Absorbance values have been normalized.

band at 1911 cm$^{-1}$ was formed within 1 ns which decayed with a time constant of 4.5 ± 0.5 ns and the bleaching recovered partially with a time constant of 3.0 ± 0.5 ns (Figure 14). The spectrum under H$_2$ at later times, $\Delta t$ = 20 $\mu$s (Figure 13b), superficially resembles the spectrum obtained under argon; however, close inspection shows that the broad band at ~1971 cm$^{-1}$ is much more intense relative to the parent bleach in the spectrum under hydrogen. Furthermore, the band at 1971 cm$^{-1}$ grew in significantly more quickly (ca. 700 ns) under hydrogen in comparison to the results obtained under argon (ca. 11 $\mu$s). These results are consistent with the formation of **2** and its isomers as a result of the reaction of [Ru(PPh$_3$)$_2$(CO)(H)$_2$] with dihydrogen after PPh$_3$ loss. The formation of some of the dimeric ruthenium species under these conditions cannot be excluded, since the $\nu$(CO) bands of **2** and the dimeric species have been shown to overlap in the low-temperature FTIR experiments above.

*TRIR of 1 in the Presence of Added Pyridine under Ar.* The TRIR spectra obtained after 355 nm irradiation of a solution of **1** in C$_6$D$_6$ with added pyridine (ca. 10$^{-2}$ M) do not show the presence of the band at 1971 cm$^{-1}$, indicating that neither the dimeric product nor **2** is formed under these conditions. However, a clear band at 1915−1920 cm$^{-1}$ with shoulders both to lower and higher wavenumbers grows in over 100 ns and is assigned to complex **4-CN** or its isomers arising from the reaction of [Ru(PPh$_3$)$_2$(CO)(H)$_2$] with pyridine. This band remains unchanged out to 28 $\mu$s (see the Supporting Information).

*TRIR of 1 in the Presence of Added Pyridine under H$_2$.* The TRIR spectra obtained after irradiation at 355 nm of a solution of **1** in C$_6$D$_6$ with added pyridine (ca. 10$^{-2}$ M) under H$_2$
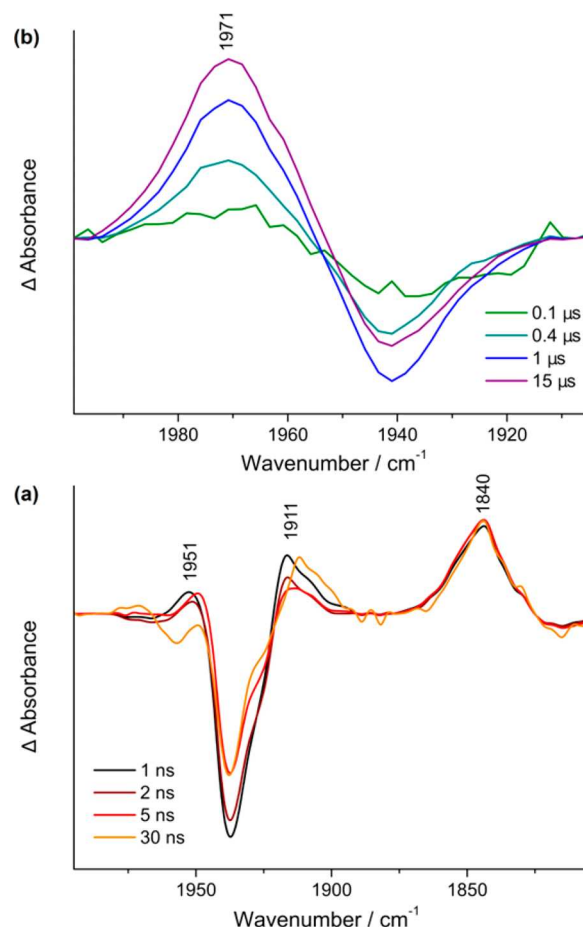


**Figure 13.** TRIR difference spectra obtained in the ranges (a) 1−30 ns and 1900−2000 cm$^{-1}$ and (b) 0.1−15 $\mu$s and 1800−2000 cm$^{-1}$ after a 355 nm laser flash of a solution of **1** in C$_6$D$_6$ under H$_2$ (ca. 1.5 atm).
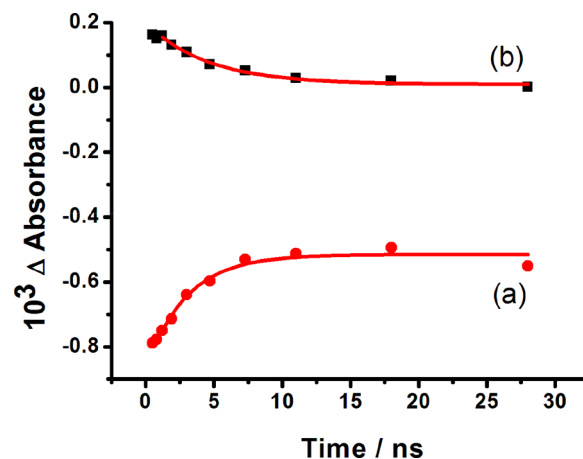


**Figure 14.** Kinetic plots at early times for (a) bleach recovery of **1** under H$_2$ at 1938 cm$^{-1}$, $\tau$ = 3.0 ± 0.5 ns, and (b) loss of 1911 cm$^{-1}$ band assigned to [Ru(CO)(PPh$_3$)$_2$(H)$_2$], $\tau$ = 4.5 ± 0.5 ns. Conditions as for Figure 13.

pressure (ca. 1 atm) showed a negative band for **1** at the earliest time (0.5 ns) and a band of [Ru(PPh$_3$)$_3$(CO)] as observed in all the earlier experiments. Additionally, the band at 1951 cm$^{-1}$ is detected at early times. Two new bands grew in over 70 ns at 1912 and 1975 cm$^{-1}$ (Figure 15a). The band at 1912 cm$^{-1}$ is assigned to the formation of complex **4-PP** or isomers, while
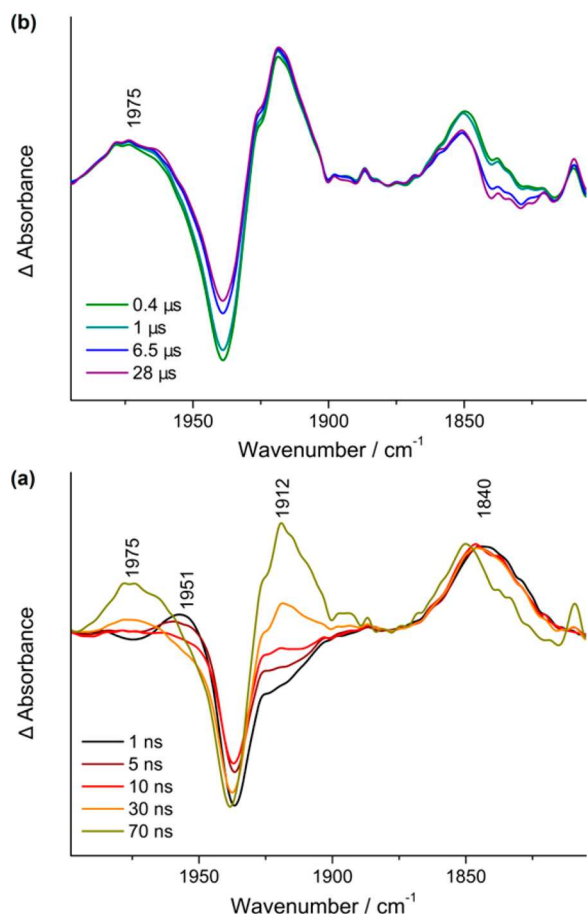
**Figure 15.** TRIR difference spectra obtained in the ranges (a) 1−70 ns and 1800−2000 cm⁻¹ (b) 0.4−28 μs after a 355 nm laser flash of a solution of **1** in $C_6D_6$ with added pyridine (ca. $10^{-2}$ M) under 1 atm of $H_2$.

the remaining band coincides with those of complex **2** and the dimer. The band at 1840 cm⁻¹ decreases and gives way to a band at 1851 cm⁻¹, which may be assigned to Ru(PPh₃)₃(CO)-(py). On a longer time scale, these bands are stable (Figure 15b).

## DISCUSSION

The NMR results discussed above differ from our earlier studies in that we see evidence for photochemical loss of both $H_2$ and of PPh₃. In the presence of $H_2$ we see formation of dihydrogen complex **2**, while in the presence of triphenylarsine we observe formation of **3**. Use of pyridine as the incoming ligand yields **4-CN** and its isomers. The low-temperature FTIR and room-temperature TRIR experiments show both intermediates and products consistent with this evidence.

**NMR Results.** The behavior of the pyridine isomers is unusual; it might be expected that the initial product would be **4-CN** with *trans* PPh₃ ligands, but the major product at low temperature is **4-PP**. Formation of **4-PP** requires dissociation of PPh₃ and rearrangement of the five-coordinate intermediate [Ru((H)₂(CO)(PPh₃)₂] to bring the PPh₃ ligands into a *cis* orientation. The rearrangement is likely to take place either in an electronic excited state or in a vibrational excited state, as has been documented in detail for Fe(CO)₄ and Cr(CO)₅.[14,50−55] Initial loss of PPh₃ *trans* to hydride followed by two successive Berry pseudorotations and coordination of pyridine would

generate **4-PP**. The surprising feature is that this process is selective for **4-PP**. The isomer **4-PP** rearranges thermally to **4-CN**. Two further isomers of the pyridine complexes **4-NP** and **4-CP** are formed as minor photoproducts. All of the isomers are accessible by a single trigonal twist starting from **4-PP** (see the Supporting Information).[56,57] Alternatively, they may occur by isomerization to a dihydrogen complex, followed by a Berry pseudorotation.

It may be asked why parallel isomerization processes are not observed for **2** and **3**. In the case of **2**, we have evidence for rapid exchange of dihydride and dihydrogen ligands which causes rapid conversion to the most stable isomer. For **3**, there is evidence for two further isomers on irradiation with multiple laser shots that are analogues of **4-NP** and **4-CP** (see the Supporting Information), but the experiments are limited by the solubility of AsPh₃ at low temperature.

The observation of hyperpolarized hydride ligand signals for **3** and **4** on photolysis requires both the substitution of PPh₃ by incoming ligand and reductive elimination of $H_2$ followed by oxidative addition of p-$H_2$. Considering the short lifetime of hyperpolarized **1**, it is likely that PPh₃ substitution occurs first. We have shown that **3** and **4** undergo thermal exchange with p-$H_2$ and they may also undergo photochemical exchange. The mechanism of this thermal exchange may involve loss of AsPh₃ or pyridine from **3** or **4**, respectively, followed by formation of **2**, intramolecular exchange of hydrogens, and recoordination of the ligand, as proposed for related iridium complexes.[58] Alternatively and more simply, **3** and **4** may be converted to dihydrogen isomers which undergo exchange with p-$H_2$ and regeneration of the initial structure.

**IR Results.** The IR spectra and reactivity of the Ru(0) intermediate [Ru(PPh₃)₃(CO)] are consistent with a single isomer of this species. On the other hand, the IR spectra point to the formation of at least two isomers of the Ru(II) intermediate [Ru(H)₂(CO)(PPh₃)₂] (Scheme 6).

We have investigated the assignments further by use of Timney ligand effect constants[59] and by estimating the CO

**Scheme 6. Summary of TRIR Observations with Experimental IR Wavenumbers for ν(CO)**
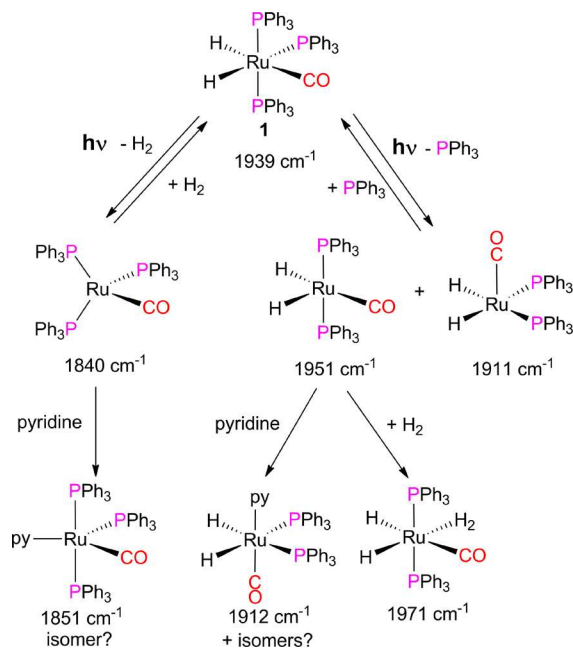
stretching frequencies by DFT methods (Table 1). The ligand effect constant for PPh$_3$ *cis* to CO is negative while that for

### Table 1. Wavenumbers of $\nu$(CO) Bands (cm$^{-1}$)

| | $\nu$(CO) | | |
|---|---|---|---|
| complex | exptl in C$_6$D$_6$ | calcd by Timney method[a] | calcd by DFT[b] |
| **1** | 1939 | 1947 | 1927 |
| **2** | 1971 | 1971 | 1974 |
| spy Ru(H)$_2$(CO)(PPh$_3$)$_2$ vacancy *trans* to H[c] | 1951 | 1960 | 1973 |
| spy Ru(H)$_2$(CO)(PPh$_3$)$_2$ vacancy *trans* to CO[c] | 1911 | 1925 | |
| Ru(CO)(PPh$_3$)$_3$ sq planar[c] | - | 1923 | |
| Ru(CO)(PPh$_3$)$_3$ butterfly | 1840 | 1842 | 1903 |

[a]Reference 59. [b]M06/LACVP(d) with 0.96 scaling. [c]Abbreviations: spy, square pyramidal; sq, square.

*trans*-PPh$_3$ is positive; thus, values of $\nu$(CO) will be very sensitive to the OC−Ru−P angle. The values for hydride are positive for both *cis* and *trans* geometries and greatly exceed the values for the other ligands. The Timney calculations are consistent with a butterfly structure for [Ru(PPh$_3$)$_3$CO] and two isomers of square-pyramidal [Ru(CO)(PPh$_3$)$_2$(H)$_2$]. Loss of PPh$_3$ *trans* to hydride without rearrangement of the skeleton of **1** should cause a high-frequency shift in $\nu$(CO) with respect to **1**, whereas rearrangement to an isomer with mutually *cis* hydrides and CO *trans* to a vacancy should cause a shift to lower frequency in comparison to that of **1**. The corresponding DFT calculations are summarized in Table 1. In light of these calculations, we deduce that PPh$_3$ photoejection does indeed generate two isomers of [Ru(H)$_2$(CO)(PPh$_3$)$_2$].

The $\nu$(CO) band of dihydrogen complex **2** is reproduced very accurately by both calculation methods; the high-frequency shift is consistent with the expected $\pi$-acceptor characteristics. The values for pyridine complexes **4-CN** and **4-PP** pose greater problems (see the Supporting Information).

The intermediate [Ru(H)$_2$(CO)(PPh$_3$)$_2$] is much more reactive than [Ru(PPh$_3$)$_3$(CO)], and we anticipate that it will react with incoming substrates to generate isomeric products. The nanosecond TRIR spectra showed strong evidence for partial in-cage recombination of PPh$_3$ with [Ru(H)$_2$(CO)-(PPh$_3$)$_2$] with a time constant of ca. 5 ns. The reaction of this species with H$_2$ under 1.5 atm (the solubility of H$_2$ in benzene is 2.9 × 10$^{-3}$ mol dm$^{-3}$ atm$^{-1}$)[60] took place with $\tau \approx$ 700 ns, while the reaction with pyridine occurred with $\tau \approx$ 70 ns at 10$^{-2}$ mol dm$^{-3}$ pyridine, indicating higher reactivity toward pyridine than toward H$_2$. The reaction of [Ru(PPh$_3$)$_3$(CO)] with H$_2$ is considerably slower ($\tau$ ca. 3 $\mu$s at the same pressure).

### ■ CONCLUSIONS

The evidence from in situ photochemistry of **1** with both NMR and IR detection that PPh$_3$ loss competes with H$_2$ reductive elimination is very strong indeed. When we first obtained NMR evidence for PPh$_3$ substitution by H$_2$ to form Ru(H)$_2$($\eta^2$-H$_2$)(CO)(PPh$_3$)$_2$ (**2**), the experiments seemed to conflict with our earlier TRIR experiments.[15] However, with the improved performance of modern TRIR experiments, it is now evident that we missed this reaction because of the need for NMR spectroscopy at low temperature and TRIR spectroscopy with greater sensitivity and time resolution. Our NMR experiments

indicate that the quantum yields for PPh$_3$ loss and H$_2$ reductive elimination are approximately equal on 355 nm photolysis.

The TRIR experiments allow characterization of coordinatively unsaturated [Ru(PPh$_3$)$_3$(CO)] and two isomers of [Ru(H)$_2$(CO)(PPh$_3$)$_2$] via their $\nu$(CO) bands. They also demonstrate that [Ru(H)$_2$(CO)(PPh$_3$)$_2$] is considerably more reactive toward H$_2$ than [Ru(PPh$_3$)$_3$(CO)]. The reaction of [Ru(PPh$_3$)$_3$(CO)] with *p*-H$_2$ generates **1** in hyperpolarized form, but this species relaxes quickly and does not exchange with *p*-H$_2$ and consequently can only be detected if the laser pulse is synchronized with the rf pulse from the NMR spectrometer. The reaction of [Ru(H)$_2$(CO)(PPh$_3$)$_2$] with H$_2$ generates the dihydrogen complex Ru(H)$_2$($\eta^2$-H$_2$)(CO)-(PPh$_3$)$_2$ (**2**). Its short $T_1$ value provides a route to relaxation of *p*-H$_2$ to thermal equilibrium of *o*-H$_2$ and *p*-H$_2$; however, its formation and the fast relaxation process can be suppressed by addition of other ligands. Reaction of AsPh$_3$ in the presence of *p*-H$_2$ generates hyperpolarized Ru(H)$_2$(AsPh$_3$)(CO)(PPh$_3$)$_2$ (**3**). The reaction of [Ru(H)$_2$(CO)(PPh$_3$)$_2$] with pyridine is more complex. Use of low-temperature methods shows that the initial product is Ru(H)$_2$(CO)(PPh$_3$)$_2$(pyridine) (**4-PP**) with a planar Ru(H)$_2$(PPh$_3$)$_2$ core and pyridine *trans* to CO. This species rearranges on warming to **4-CN**, the pyridine analogue of complexes **2** and **3**. Two more isomers, **4-NP** and **4-CP**, are formed in low yield. Under an atmosphere of *p*-H$_2$, all four isomers are detected in hyperpolarized form. Unlike the case for **1**, complexes **3** and **4-CN** undergo thermal exchange at room temperature with *p*-H$_2$.

### ■ EXPERIMENTAL SECTION

Complex **1** was prepared using the old procedure reported in the literature.[61] Chemical manipulations and sample preparations were carried out under inert-atmosphere conditions using standard Schlenk (vacuum 10$^{-2}$ mbar) or high-vacuum methods (10$^{-4}$ mbar). *p*-H$_2$ was generated by cooling hydrogen gas over charcoal in a copper block at ca. 30 K. The proportion of *p*-H$_2$ at 30 K was calculated as >99%. Pressures of *p*-H$_2$ were measured with an MKS Baratron capacitance manometer. Deuterated solvents for use in NMR were degassed and dried before use; benzene-$d_6$ and toluene-$d_8$ were obtained from Aldrich and dried on potassium mirrors in ampules fitted with a greaseless tap. $^{15}N$-Pyridine (Aldrich) was used as received.

**NMR Measurements. Ex Situ UV Photolysis Setup.** Photochemical reactions were performed with an Oriel 350 W high-pressure xenon arc lamp. Unwanted heating was minimized by use of a water filter of 10 cm length between the sample and the lamp.

**Continuous Wave Laser Experiments.** The in situ photolysis equipment has been described before.[62] In summary, in situ photolysis experiments were performed using a wide-bore Bruker DRX-400 NMR spectrometer equipped with a 63 mW Kimmon IK series He−Cd laser at 325 nm. The laser beam was directed into the sample in the spectrometer through the air gap between the magnet bore and a narrow-bore probe. The sample was cooled using a liquid N$_2$ boil-off evaporator. The laser was mounted on a specially designed platform situated in front of the NMR spectrometer that could be adjusted both horizontally and vertically. The laser alignment was optimized by using an NMR sample of Ru(CO)$_3$(dppe) (dppe = Ph$_2$PCH$_2$CH$_2$PPh$_2$) in deuterated toluene, pressurized with *p*-H$_2$. On exposure to UV light the sample reacts with *p*-H$_2$ to generate enhanced resonances arising from Ru(H)$_2$(CO)$_3$(dppe). Continuous recording of the spectra allowed the optimal position of the laser beam to be identified.

**Pulsed Laser Experiments.** All NMR spectra were recorded on a Bruker Avance II 600 MHz spectrometer with a 14 T wide-bore magnet fitted with a 5 mm BBO probe. In situ laser photolysis was carried out with a pulsed Nd:YAG laser (Continuum Surelite II) fitted with a frequency-tripling crystal (output 355 nm). Operating conditions were typically as follows: 10 Hz repetition rate, flash

lamp voltage 1.49 kV, and Q-switch delay increased from the standard to 320 $\mu$s yielding a laser power of 75 mW in internal mode. The energy of a single laser pulse was measured using an energy meter calibrated for 355 nm to be ~29.8 mJ under our operating conditions (external triggering with Q-switch delay set to 150 $\mu$s). The unfocused laser beam is directed at the base of the spectrometer and reflected up into the probe via a mirror as previously reported.[32] Adjustment screws control the vertical and horizontal position of the mirror, which is on a kinematic mount. The system is fully shielded from the operator, and the screws of the kinematic mount can be adjusted from outside the shield. The laser radiation is incident on a fixed mirror that is level with the sample and passes through a hole in the probe onto the NMR tube. Standard NMR tubes fitted with Young taps were used. The samples contained 1−2 mg of compound ($Abs_{355} \approx 0.7$) and approximately 0.4 mL of solvent. A sample of $Ru(dppe)_2H_2$ in $C_6D_6$ was used for laser alignment with $p$-$H_2$ amplification in real time. Standard NMR pulse sequences were modified for use with $p$-$H_2$ by including a synchronized laser initiation sequence prior to NMR excitation. A purpose-written program was used to control the laser firing from the NMR console with the laser set on external triggering. The program sets the laser to fire one warm-up shot before the fire signal. The NMR pulse was initiated at a set delay time ($\tau$) following the fire signal. The intrinsic time delay between sending the fire signal from the spectrometer and the actual firing of the laser pulse was measured with a photodiode and an oscilloscope to be 150 $\mu$s (equal to the Q-switch delay for the generation of the pulse). This signal delay was incorporated into the pulse sequence such that synchronized measurements with a time delay, $\tau$, were achieved by setting the spectrometer delay to $\tau + 150$ $\mu$s. The precision of this delay between the laser and radio frequency (rf) pulses was controlled by the 200 ns clock of the spectrometer.

**TRIR Measurements.** Our time-resolved infrared (TRIR) measurements were based on a pump−probe method that has been described in detail previously.[30,63] In brief, the probe source is a broadband mid-IR pulse with 100 fs duration (fwhm) and around 1 $\mu$J energy at 1 kHz. The pump source is the third harmonic output (355 nm) of a Q-switched Nd:YVO laser with 0.5 ps duration (fwhm) and around 3 $\mu$J energy and is synchronized to the probe pulse. The delay between pump and probe pulses can be controlled with a pulse generator (DG535, Stanford Research System) from 0.5 ns to 100 $\mu$s. The broad-band transmitted probe pulse is detected with a 128-element HgCdTe array detector. The sample solutions were flowed through a $CaF_2$-windowed IR cell, path length 0.25 mm, which was rastered in two dimensions at high speed to reduce overheating and degradation of the sample solution. All spectral and kinetic fitting procedures were carried out using Microcal Origin 7 software.

**Low-Temperature Photolysis.** The low-temperature photolysis IR experiments were performed in a manner similar to that described previously.[64] The high-pressure−low-temperature (HP-LT) cell used in the low-temperature experiments has been described in detail elsewhere.[65] Briefly, the HP-LT cell was filled with a solution of **1** dissolved in toluene-$d_8$. Toluene-$d_8$ was used to minimize IR solvent background issues and to permit low-temperature experiments in solution because of its lower freezing point in comparison to that of benzene-$d_6$. The cell was attached to a cold finger of a cryogenic cooling system and cooled to the required temperature (220 K). The photolysis source used in these experiments was a Philips HPK 125W medium-pressure mercury arc lamp, which provided broad-band UV and visible light. IR spectra were recorded using a Nicolet 730 interferometer linked to a computer running Omnic software.

**IR Spectroscopy.** Other IR spectra were recorded on a Mattson Unicam RS FTIR instrument, connected to a PC running WINFIRST software, or a Nicolet Nexus apparatus, connected to a PC running Omnic E.S.P. 5.2 software.

**UV−Vis Spectroscopy.** UV−vis spectra were recorded on a Perkin-Lambda 7 spectrometer, using a PC running PECSS software.

**DFT Calculations.** Density functional theory calculations were used to optimize geometries and simulate harmonic vibrational frequencies for several of the complexes (see the Supporting Information). Preliminary calculations of the parent species performed

with the Stuttgart relativistic small core pseudopotential and basis set mixed with the 6-311G(d) basis set for nonmetal atoms,[66] and using the B3LYP,[67,68] PBE0,[69] and M06[70] functionals, representing 20, 25, and 27% HF exchange, respectively, found that M06 gave the closest match with experiment. Consequently, the M06 level of theory within the Q-Chem quantum-chemical software package was adopted for fuller calculations.[71] Calculations were converged then using the double-$\zeta$ 6-31G(d) basis set for C, N, O, P, and H atoms and the quasi-relativistic LANL2DZ pseudopotential and basis set for Ru.[72] This combination has been labeled as LACVP(d). Optimized geometries were confirmed by the absence of imaginary frequencies, and these harmonic frequencies have been scaled by a uniform factor of 0.96 to account for anharmonic and experimental effects.[73]

## ■ ASSOCIATED CONTENT

**ⓢ Supporting Information**

The Supporting Information is available free of charge on the ACS Publications website at DOI: 10.1021/acs.organo-met.7b00802. Experimental datasets associated with this paper were deposited with Univ. of York library.

> NMR spectra, pulse sequences used in laser pump-NMR probe experiments, $T_1$(min) relaxation, TRIR difference spectra, FTIR spectra, DFT calculated structures and CO-stretching frequencies, and calculated and observed $\nu$(CO) values for pyridine complexes (PDF)

## ■ AUTHOR INFORMATION

**Corresponding Authors**
*E-mail for S.B.D.: simon.duckett@york.ac.uk.
*E-mail for M.W.G.: mike.george@nottingham.ac.uk.
*E-mail for R.N.P.: robin.perutz@york.ac.uk.

**ORCID** ⓞ
Barbara Procacci: 0000-0001-7044-0560
Simon B. Duckett: 0000-0002-9788-6615
Michael W. George: 0000-0002-7844-1696
Magnus W. D. Hanson-Heine: 0000-0002-6709-297X
Raphael Horvath: 0000-0002-2695-4895
Robin N. Perutz: 0000-0001-6286-0282
Khuong Q. Vuong: 0000-0001-9558-9273

**Notes**
The authors declare no competing financial interest.

## ■ ACKNOWLEDGMENTS

## ■ REFERENCES

(1) Crossley, S. W. M.; Obradors, C.; Martinez, R. M.; Shenvi, R. A. *Chem. Rev.* **2016**, *116*, 8912−9000.

(2) Maity, A.; Teets, T. S. *Chem. Rev.* **2016**, *116*, 8873−911.

(3) Rossin, A.; Peruzzini, M. *Chem. Rev.* **2016**, *116*, 8848−72.

(4) Perutz, R. N.; Procacci, B. *Chem. Rev.* **2016**, *116*, 8506−44.

(5) Geoffroy, G. L.; Bradley, M. G. *Inorg. Chem.* **1977**, *16*, 744−8.

(6) Wakatsuki, Y.; Yamazaki, H.; Kumegawa, N.; Satoh, T.; Satoh, J. Y. *J. Am. Chem. Soc.* **1991**, *113*, 9604−10.

(7) Wakatsuki, Y.; Yamazaki, H.; Maruyama, Y.; Shimizu, I. *J. Chem. Soc., Chem. Commun.* **1991**, 261−3.

(8) Du, H. G.; Liu, Q.; Shi, S. J.; Zhang, S. W. *J. Organomet. Chem.* **2001**, *627*, 127−31.

(9) Samouei, H.; Grushin, V. V. *Organometallics* **2013**, *32*, 4440−3.

(10) Arockiam, P. B.; Bruneau, C.; Dixneuf, P. H. *Chem. Rev.* **2012**, *112*, 5879−918.

(11) Kakiuchi, F.; Murai, S. *Acc. Chem. Res.* **2002**, *35*, 826−34.

(12) Nixon, T. D.; Whittlesey, M. K.; Williams, J. M. J. *Dalton Trans.* **2009**, 753−62.

(13) Naota, T.; Takaya, H.; Murahashi, S. I. *Chem. Rev.* **1998**, *98*, 2599−660.

(14) Perutz, R. N.; Torres, O.; Vlček, A. J. *Photochemistry of Metal Carbonyls*; Reedijk, J., Poeppelmeier, K., Eds.; Elsevier: Oxford, U.K., 2013; Comprehensive Inorganic Chemistry II, Vol. 8, Chapter 8.06, pp 229−53.

(15) Colombo, M.; George, M. W.; Moore, J. N.; Pattison, D. I.; Perutz, R. N.; Virrels, I. G.; Ye, T. Q. *J. Chem. Soc., Dalton Trans.* **1997**, 2857−9.

(16) Torres, O.; Calladine, J. A.; Duckett, S. B.; George, M. W.; Perutz, R. N. *Chem. Sci.* **2015**, *6*, 418−24.

(17) Calladine, J. A.; Torres, O.; Anstey, M.; Ball, G. E.; Bergman, R. G.; Curley, J.; Duckett, S. B.; George, M. W.; Gilson, A. I.; Lawes, D. J.; Perutz, R. N.; Sun, X. Z.; Vollhardt, K. P. C. *Chem. Sci.* **2010**, *1*, 622−30.

(18) Calladine, J. A.; Duckett, S. B.; George, M. W.; Matthews, S. L.; Perutz, R. N.; Torres, O.; Khuong, Q. V. *J. Am. Chem. Soc.* **2011**, *133*, 2303−10.

(19) Godard, C.; Callaghan, P.; Cunningham, J. L.; Duckett, S. B.; Lohman, J. A. B.; Perutz, R. N. *Chem. Commun.* **2002**, 2836−7.

(20) Blazina, D.; Dunne, J. P.; Aiken, S.; Duckett, S. B.; Elkington, C.; McGrady, J. E.; Poli, R.; Walton, S. J.; Anwar, M. S.; Jones, J. A.; Carteret, H. A. *Dalton Trans.* **2006**, 2072−80.

(21) Geftakis, S.; Ball, G. E. *J. Am. Chem. Soc.* **1998**, *120*, 9953−4.

(22) Lawes, D. J.; Geftakis, S.; Ball, G. E. *J. Am. Chem. Soc.* **2005**, *127*, 4134−5.

(23) Ball, G. E.; Brookes, C. M.; Cowan, A. J.; Darwish, T. A.; George, M. W.; Kawanami, H. K.; Portius, P.; Rourke, J. P. *Proc. Natl. Acad. Sci. U. S. A.* **2007**, *104*, 6927−32.

(24) Lawes, D. J.; Darwish, T. A.; Clark, T.; Harper, J. B.; Ball, G. E. *Angew. Chem., Int. Ed.* **2006**, *45*, 4486−90.

(25) Young, R. D.; Hill, A. F.; Hillier, W.; Ball, G. E. *J. Am. Chem. Soc.* **2011**, *133*, 13806−9.

(26) Ampt, K. A. M.; Burling, S.; Donald, S. M. A.; Douglas, S.; Duckett, S. B.; Macgregor, S. A.; Perutz, R. N.; Whittlesey, M. K. *J. Am. Chem. Soc.* **2006**, *128*, 7452−3.

(27) Montiel-Palma, V.; Perutz, R. N.; George, M. W.; Jina, O. S.; Sabo-Etienne, S. *Chem. Commun.* **2000**, 1175−6.

(28) Calladine, J. A.; Horvath, R.; Davies, A. J.; Wriglesworth, A.; Sun, X. Z.; George, M. W. *Appl. Spectrosc.* **2015**, *69*, 519−24.

(29) Greetham, G. M.; Burgos, P.; Cao, Q. A.; Clark, I. P.; Codd, P. S.; Farrow, R. C.; George, M. W.; Kogimtzis, M.; Matousek, P.; Parker, A. W.; Pollard, M. R.; Robinson, D. A.; Xin, Z. J.; Towrie, M. *Appl. Spectrosc.* **2010**, *64*, 1311−9.

(30) Towrie, M.; Grills, D. C.; Dyer, J.; Weinstein, J. A.; Matousek, P.; Barton, R.; Bailey, P. D.; Subramaniam, N.; Kwok, W. M.; Ma, C. S.; Phillips, D.; Parker, A. W.; George, M. W. *Appl. Spectrosc.* **2003**, *57*, 367−80.

(31) Banister, J. A.; George, M. W.; Grubert, S.; Howdle, S. M.; Jobling, M.; Johnson, F. P. A.; Morrison, S. L.; Poliakoff, M.; Schubert, U.; Westwell, J. R. *J. Organomet. Chem.* **1994**, *484*, 129−35.

(32) Torres, O.; Procacci, B.; Halse, M. E.; Adams, R. W.; Blazina, D.; Duckett, S. B.; Eguillor, B.; Green, R. A.; Perutz, R. N.; Williamson, D. C. *J. Am. Chem. Soc.* **2014**, *136*, 10124−31.

(33) Pravdivtsev, A. N.; Yurkovskaya, A. V.; Petrov, P. A.; Vieth, H. M. *Phys. Chem. Chem. Phys.* **2017**, *19*, 25961.

(34) Levison, J. J. *J. Chem. Soc. A* **1970**, 639−43.

(35) Perutz, R. N.; Sabo-Etienne, S. *Angew. Chem., Int. Ed.* **2007**, *46*, 2578−92.

(36) Luo, X. L.; Crabtree, R. H. *J. Am. Chem. Soc.* **1990**, *112*, 6912−8.

(37) Crabtree, R. H. *Chem. Rev.* **2016**, *116*, 8750−69.

(38) Gusev, D. G.; Vymenits, A. B.; Bakhmutov, V. I. *Inorg. Chim. Acta* **1991**, *179*, 195−201.

(39) Samouei, H.; Miloserdov, F. M.; Escudero-Adan, E. C.; Grushin, V. V. *Organometallics* **2014**, *33*, 7279−83.

(40) Riddlestone, I. M.; McKay, D.; Gutmann, M. J.; Macgregor, S. A.; Mahon, M. F.; Sparkes, H. A.; Whittlesey, M. K. *Organometallics* **2016**, *35*, 1301−12.

(41) Grellier, M.; Mason, S. A.; Albinati, A.; Capelli, S. C.; Rizzato, S.; Bijani, C.; Coppel, Y.; Sabo-Etienne, S. *Inorg. Chem.* **2013**, *52*, 7329−37.

(42) Hebden, T. J.; Goldberg, K. I.; Heinekey, D. M.; Zhang, X. W.; Emge, T. J.; Goldman, A. S.; Krogh-Jespersen, K. *Inorg. Chem.* **2010**, *49*, 1733−42.

(43) Morris, R. H. *Coord. Chem. Rev.* **2008**, *252*, 2381−94.

(44) Sleigh, C. J.; Duckett, S. B.; Mawby, R. J.; Lowe, J. P. *Chem. Commun.* **1999**, 1223−4.

(45) The dimer observed by TRIR spectroscopy offers a potential route to formation of Ru(H)$_2$(PPh$_3$)$_2$(CO)$_2$; see IR Studies.

(46) Ball, G. E.; Mann, B. E. *J. Chem. Soc., Chem. Commun.* **1992**, 561−3.

(47) Aguilar, J. A.; Elliott, P. I. P.; Lopez-Serrano, J.; Adams, R. W.; Duckett, S. B. *Chem. Commun.* **2007**, 1183−5.

(48) Abdur-Rashid, K.; Abbel, R.; Hadzovic, A.; Lough, A. J.; Morris, R. H. *Inorg. Chem.* **2005**, *44*, 2483−92.

(49) Halse, M. E.; Procacci, B.; Henshaw, S. L.; Perutz, R. N.; Duckett, S. B. *J. Magn. Reson.* **2017**, *278*, 25−38.

(50) Besora, M.; Carreon-Macedo, J. L.; Cimas, A.; Harvey, J. N. *Adv. Inorg. Chem.* **2009**, *61*, 573−623.

(51) Kosma, K.; Trushin, S. A.; Fuss, W.; Schmid, W. E.; Schneider, B. M. R. *Phys. Chem. Chem. Phys.* **2010**, *12*, 13197−214.

(52) Trushin, S. A.; Fuss, W.; Kompa, K. L.; Schmid, W. E. *J. Phys. Chem. A* **2000**, *104*, 1997−2006.

(53) Paterson, M. J.; Hunt, P. A.; Robb, M. A.; Takahashi, O. *J. Phys. Chem. A* **2002**, *106*, 10494−504.

(54) Portius, P.; Yang, J. X.; Sun, X. Z.; Grills, D. C.; Matousek, P.; Parker, A. W.; Towrie, M.; George, M. W. *J. Am. Chem. Soc.* **2004**, *126*, 10713−20.

(55) Burdett, J. K.; Grzybowski, J. M.; Perutz, R. N.; Poliakoff, M.; Turner, J. J.; Turner, R. F. *Inorg. Chem.* **1978**, *17*, 147−54.

(56) Soubra, C.; Oishi, Y.; Albright, T. A.; Fujimoto, H. *Inorg. Chem.* **2001**, *40*, 620−7.

(57) Rodger, A.; Johnson, B. F. G. *Inorg. Chem.* **1988**, *27*, 3061−2.

(58) Ruddlesden, A. J.; Mewis, R. E.; Green, G. G. R.; Whitwood, A. C.; Duckett, S. B. *Organometallics* **2015**, *34*, 2997−3006.

(59) Timney, J. A. *Inorg. Chem.* **1979**, *18*, 2502−6.

(60) Wilhelm, E.; Battino, R. *Chem. Rev.* **1973**, *73*, 1−9.

(61) Ahmad, N.; Uttley, M. F.; Robinson, S. D. *J. Chem. Soc., Dalton Trans.* **1972**, 843−7.

(62) Clark, J. L.; Duckett, S. B. *Dalton Trans.* **2014**, *43*, 1162−71.

(63) Brennan, P.; George, M. W.; Jina, O. S.; Long, C.; McKenna, J.; Pryce, M. T.; Sun, X. Z.; Vuong, K. Q. *Organometallics* **2008**, *27*, 3671−80.

(64) Childs, G. I.; Colley, C. S.; Dyer, J.; Grills, D. C.; Sun, X. Z.; Yang, J. X.; George, M. W. *J. Chem. Soc., Dalton Trans.* **2000**, 1901−6.

(65) Cooper, A. I.; Poliakoff, M. *Chem. Phys. Lett.* **1993**, *212*, 611−6.

(66) Dolg, M.; Wedig, U.; Stoll, H.; Preuss, H. *J. Chem. Phys.* **1987**, *86*, 866−72.

(67) Becke, A. D. *J. Chem. Phys.* **1993**, *98*, 5648−52.

(68) Stephens, P. J.; Devlin, F. J.; Chabalowski, C. F.; Frisch, M. J. *J. Phys. Chem.* **1994**, *98*, 11623−7.

(69) Adamo, C.; Barone, V. *J. Chem. Phys.* **1999**, *110*, 6158−70.

(70) Zhao, Y.; Truhlar, D. G. *Theor. Chem. Acc.* **2008**, *120*, 215−41.

(71) Shao, Y. H.; Gan, Z. T.; Epifanovsky, E.; Gilbert, A. T. B.; Wormit, M.; Kussmann, J.; Lange, A. W.; Behn, A.; Deng, J.; Feng, X. T.; Ghosh, D.; Goldey, M.; Horn, P. R.; Jacobson, L. D.; Kaliman, I.; Khaliullin, R. Z.; Kus, T.; Landau, A.; Liu, J.; Proynov, E. I.; Rhee, Y. M.; Richard, R. M.; Rohrdanz, M. A.; Steele, R. P.; Sundstrom, E. J.; Woodcock, H. L.; Zimmerman, P. M.; Zuev, D.; Albrecht, B.; Alguire, E.; Austin, B.; Beran, G. J. O.; Bernard, Y. A.; Berquist, E.; Brandhorst, K.; Bravaya, K. B.; Brown, S. T.; Casanova, D.; Chang, C. M.; Chen, Y. Q.; Chien, S. H.; Closser, K. D.; Crittenden, D. L.; Diedenhofen, M.;

DiStasio, R. A.; Do, H.; Dutoi, A. D.; Edgar, R. G.; Fatehi, S.; Fusti-Molnar, L.; Ghysels, A.; Golubeva-Zadorozhnaya, A.; Gomes, J.; Hanson-Heine, M. W. D.; Harbach, P. H. P.; Hauser, A. W.; Hohenstein, E. G.; Holden, Z. C.; Jagau, T. C.; Ji, H. J.; Kaduk, B.; Khistyaev, K.; Kim, J.; Kim, J.; King, R. A.; Klunzinger, P.; Kosenkov, D.; Kowalczyk, T.; Krauter, C. M.; Lao, K. U.; Laurent, A. D.; Lawler, K. V.; Levchenko, S. V.; Lin, C. Y.; Liu, F.; Livshits, E.; Lochan, R. C.; Luenser, A.; Manohar, P.; Manzer, S. F.; Mao, S. P.; Mardirossian, N.; Marenich, A. V.; Maurer, S. A.; Mayhall, N. J.; Neuscamman, E.; Oana, C. M.; Olivares-Amaya, R.; O'Neill, D. P.; Parkhill, J. A.; Perrine, T. M.; Peverati, R.; Prociuk, A.; Rehn, D. R.; Rosta, E.; Russ, N. J.; Sharada, S. M.; Sharma, S.; Small, D. W.; Sodt, A. *Mol. Phys.* **2015**, *113*, 184−215.

(72) Hay, P. J.; Wadt, W. R. *J. Chem. Phys.* **1985**, *82*, 299−310.

(73) Merrick, J. P.; Moran, D.; Radom, L. *J. Phys. Chem. A* **2007**, *111*, 11683−700.